



FeNi₃@SiO₂ magnetic nanocomposite as a highly efficient Fenton-like catalyst for humic acid adsorption and degradation in neutral environments

M. Khodadadi^{a,b}, M.H. Ehrampoush^c, A. Allahresani^d, M.T. Ghaneian^c, M.H. Lotfi^e, A.H. Mahvi^{f,g,*}

^aDepartment of Environmental Health Engineering, International Campus, Shahid Sadoughi University of Medical Sciences, Yazd, Iran, email: maryam.khodadadi@gmail.com

^bSocial Determinants of Health Research Center, Birjand University of Medical Sciences, Birjand, Iran

^cEnvironmental Sciences and Technology Research Center, Department of Environmental Health Engineering, Shahid Sadoughi University of Medical Sciences, Yazd, Iran, emails: ehrampoush@ssu.ac.ir (M.H. Ehrampoush), mtghaneian@yahoo.com (M.T. Ghaneian)

^dDepartment of Chemistry, Faculty of Science, University of Birjand, Birjand, Iran, email: a_allahresani@birjand.ac.ir

^eDepartment of Biostatistics & Epidemiology, Faculty of Health, Shahid Sadoughi University of Medical Sciences, Yazd, Iran, email: mhlotfi56359@gmail.com

^fCenter for Solid Waste Research (CSWR), Institute for Environmental Research (IER), Tehran University of Medical Sciences, Tehran, Iran, email: ahmahvi@yahoo.com

^gDepartment of Environmental Health Engineering, School of Public Health, Tehran University of Medical Sciences, Tehran, Iran

Received 8 August 2017; Accepted 30 April 2018

ABSTRACT

In this research, the ability of Fenton-like catalytic process in the presence of H₂O₂ for degradation of humic acid in simulated water was studied. In this regard, FeNi₃ nanoparticles were synthesized by the coprecipitation method, using SiO₂. The properties of the prepared FeNi₃@SiO₂ were assessed using Fourier transform infrared spectroscopy, vibrating sample magnetometer, field-emission scanning electron microscopy and transmission electron microscopy. The studied parameters were pH (3, 5, 7, 9 and 11), contact time (5–180 min), nanocomposite dose (0.005–0.1 g/L), concentration of humic acid (2–15 mg/L) and concentration of H₂O₂ (50–200 mg/L). The highest removal percentage of humic acid was 100% at pH = 7, with humic acid concentration of 10 PPM, FeNi₃@SiO₂ dosage of 0.1 g/L and H₂O₂ dosage of 200 mg/L. According to the results, the Fenton-like catalytic process of FeNi₃@SiO₂/H₂O₂ had high efficiency in removing humic acid from aquatic environment.

Keywords: FeNi₃@SiO₂ magnetic nanoparticles; Humic acid; Catalyst; Fenton-like; Advanced oxidation process

1. Introduction

Almost all surface waters contain natural organic matters (NOMs) which are complex compounds of organic matter resulting from the chemical and biological decomposition of plants and animals in water bodies. NOMs are mostly complex compounds of various organic matters, for example,

bacteria, viruses, humic and folic acids, polysaccharides and proteins.

The presence of NOM in drinking water causes problems in most water treatment processes, thereby decreasing the quality of water by creating aesthetic problems such as yellow and brownish water as well as unpleasant taste and odour [1]. Moreover, the existence of these compounds in drinking water leads to numerous problems in water treatment processes, and it is essential to be removed. NOM compounds mostly consist of different parts with unique properties and

* Corresponding author.

varying molecule sizes (small to large molecules and large particles). The large difference in the size of NOM molecules creates complexities for their removal from water, especially because seasonal changes highly affect their qualities and concentrations in surface waters [1–3]. NOM mixtures are classified into hydrophilic and hydrophobic groups; the former usually includes aliphatic carbon and nitrogen compounds, for example, carboxylic acids, carbohydrates and proteins, and the latter mostly consists of humic and fulvic compounds which include aromatic carbon, phenolic circle and double bonds [4].

Humic substances (HSs) often comprise one half of NOMs [1,5]. The major constituents of HSs are aliphatic and aromatic structures as well as carboxylic and phenolic-OH groups and quinones. HSs are divided into three main groups. Humic, the first group, is completely insoluble, the second, haloacetic, being soluble in alkaline and insoluble in acidic environments, and the third group, folic acid, being soluble at all pH levels [6]. In recent years, humic acid has received considerable attention as a progenitor of disinfection by-products (DBPs) [7]. It has been shown that humic acid can be oxidized to small organic molecular compounds and may result in halogenated DBPs as a matter of drinking water disinfection process by chlorinated compounds [8]. Trihalomethanes (THMs) and haloacetic acids are among the most important DBPs, suspected to be carcinogenic and mutagenic. THMs can cause bladder, kidney and colon cancer [8,9]. According to the United States Environmental Protection Agency, the allowable concentration of THMs in drinking water is 0.08 mg/L at stage 1 of rule application and 0.03 and 0.04 mg/L at stage 2 [10,11].

Based on the noted considerations, humic acid compounds must be removed from aquatic environments prior to disinfection. So far, numerous methods have been studied for the removal of humic acid compounds from drinking water. It has been proven that the common water treatment processes, for example, coagulation, flocculation, adsorption and filtration, do not have a significant effect on the removal of humic acid. The usual removal percentage of total organic carbon in common drinking water treatment methods is approximately 10%–50% [12]. Moreover, each of these methods has certain disadvantages. For instance, the activated carbon adsorption method is quite expensive, with difficult reduction processes. Furthermore, the chemical coagulation method requires the use of chemicals which generate large amounts of sludge. The disadvantages of the ion exchange method results in consumption of chemicals and taking a large space considering the volume of generated water. Also, membrane filtration has high capital and operating costs [13–15].

Since applying advanced oxidation processes (AOPs) from active radicals has high efficiency in oxidizing organic matters, so AOPs have received considerable attention in drinking water treatment for past two decades. By forming active radicals, especially hydroxyl radicals (oxidation potential = 2.8 V), AOPs oxidize organic chemical compounds in aquatic environments. These processes can treat highly toxic matters or pollutants which cannot be easily decomposed in biological processes [16]. Hydroxyl radicals are the most important oxidizers with a high activity, which do not have a selective property in removing organic matters [17,18].

The Fenton process is a major AOP known as homogeneous Fenton process, in which H_2O_2 is decomposed in the presence of Fe^{2+} ion. Unfortunately, the Fe^{2+} - H_2O_2 process has several problems, making it hard to use; stoichiometric amounts of iron must be added to the system, which are usually oxidized to Fe^{3+} , thereby requiring complementary treatment for removal. The optimal pH for the generation of hydroxyl radical is in the range of 2–3. Therefore, a large amount of acid is needed, and neutralization must be performed after this step. In addition, large amounts of sludge are generated due to the use of ferric salts, which is harmful for the environment [18–20]. In addition, in most cases, homogeneous catalysts need external sources such as light, sonication or electrical energy to accelerate the reaction, thereby increasing the costs of such method [20]. Based on the noted points, studies have extensively examined the heterogeneous Fenton-like catalytic process based on iron (nano- or micro-sized) or other metals to reduce the limitations mentioned for Fe^{2+} - H_2O_2 [21,22].

Thus, most of the recent studies have been aimed to produce nanoparticles which could act as a Fenton-like catalytic process with acceptable efficiency in neutral conditions and with no need for any external energy source. For example, effective catalysts can be produced using iron, Fe_3O_4 , Mn_3O_4 and other particles [23]. Moreover, to overcome the problems of homogeneous Fenton process, chelating factors such as ethylene diamine tetraacetic acid, oxalate, citrate and tartrate are used to prevent the sedimentation of dissolved iron. Recently, heterogeneous Fenton-like catalytic processes using iron oxides, iron stabilized on zeolite, clay and carbonated materials have been utilized. Contrary to homogeneous catalysts, heterogeneous catalysts act in a wide range of pH [24].

Zhang et al. [25] showed that covering Fe_3O_4 nanoparticles with a thin layer of carbon as an effective catalyst in the Fenton-like process acts without any external energy source.

By covering Fe_3O_4 nanoparticles with SiO_2 and forming $Fe_3O_4@SiO_2$, Yang et al. managed to use this nanoparticle in a Fenton-like catalytic process and removed the methylene blue dye in neutral conditions. They concluded that the SiO_2 cover enhanced the catalytic activity of iron nanoparticles [18]. Liu et al. [26] utilized the $Fe_3O_4/TiO_2/C$ nanocomposite in a Fenton-like catalytic process to remove methylene blue dye. Also, the Fenton-like catalytic process of TiO_2 -doped Fe_3O_4 was investigated in the removal of dye, with maximum efficiency in neutral pH conditions [27]. Humic acid in drinking water sources has harmful effects on human health. Moreover, the use of magnetic nanocomposites in water treatment is an up-to-date research area and the AOP has high efficiency in removing organic pollutants. Therefore, in this study, first, $FeNi_3@SiO_2$ (FNS MNP_s) magnetic nanoparticles were studied and, then by determining their properties with special technique such as transmission electron microscopy (TEM), field-emission scanning electron microscopy (FESEM), Fourier transform infrared spectroscopy (FTIR) and vibrating sample magnetometer (VSM) spectra, their efficiency in removing humic acid in different conditions was examined.

2. Experimental

2.1. Chemicals

Acid humic was manufactured by Acros (Fisher Scientific). Iron(II) chloride ($FeCl_2 \cdot 4H_2O$), nickel chloride ($NiCl_2 \cdot 6H_2O$),

80% hydrazine hydrate ($N_2H_4 \cdot H_2O$), tetraethyl orthosilicate (TEOS) ($SiC_8H_{20}O_4$) and 30% H_2O_2 were purchased from Merck, Germany. Deionized water was used to prepare the solutions in all the steps.

2.2. Procedures

2.2.1. Synthesis of $FeNi_3@SiO_2$ magnetic nanoparticles

Synthesis was performed through the following steps:

- To synthesize the $FeNi_3$ nanoparticle, 1 g of polyethylene glycol (1.0 g, MW 6000) was dissolved in 180 mL of deionized water. Then, 0.713 g of $NiCl_2 \cdot 6H_2O$ and 0.1988 g of $FeCl_2 \cdot 4H_2O$ were separately dissolved in 10 cm³ of deionized water.
- pH was regulated in the range of 12–13 using NaOH.
- Then, 9.1 mL of hydrazine hydrate ($N_2H_4 \cdot H_2O$, 80% concentration) was added to the suspension. The reaction was performed for 24 h in vigorous mixing conditions. During this period, pH was maintained in the previous range. After the coprecipitation step, black $FeNi_3$ nanoparticles were separated using an N42 magnet and washed several times with deionized water so that pH would reach the neutral range. Afterwards, it was dried at 80°C in vacuum for 8 h [28].

To core-shell the SiO_2 and stabilize it on $FeNi_3$, these steps were followed: 0.5 g of the synthesized $FeNi_3$ magnetic nanoparticle was dispersed in a mixture of 80 mL of ethanol, 20 mL of deionized water and 2 mL of 28% ammonia. Then, 1 mL of TEOS was added to the previous solution dropwise and stirred at 500 rpm at ambient temperature for 24 h [29].

The resulting $FeNi_3@SiO_2$ magnetic nanoparticles (Fig. 1) were washed with water and ethanol several times and, after separation by an N42 magnet, dried in vacuum at 60°C [18,28].

2.2.2. Properties of synthesized nanocomposite

The FESEM was used to study the shape, average diameter and surface details; and to provide structural analysis (SIGMA VP-500, Zeiss, Germany). The TEM (Zeiss-EM10C-100 KV, Germany) was also used to study the sample with high resolution and magnification. The FTIR of the nanocomposite was conducted using an AVATAR, 370 FT-IR device. Magnetism was evaluated using a VSM (Model 7400 VSM) and Brunauer–Emmett–Teller (BET) using Belsorp mini II.

2.2.2.4. Experiments of humic acid removal using the $FeNi_3@SiO_2$ magnetic nanocomposite alone (adsorption) and in the presence of H_2O_2 (catalytic degradation)

To prepare the stock solution (1,000 mg/L), pure humic acid powder was utilized. This solution was kept weekly

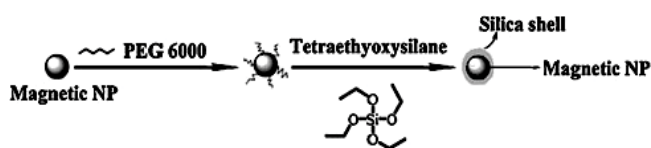


Fig. 1. Schematic representation of the synthesis of $FeNi_3@SiO_2$ magnetic nanoparticles [28].

in dark at 4°C. All the experiments were performed on 200 mL samples in a batch system at laboratory temperature ($24^\circ C \pm 2^\circ C$). To regulate pH, hydrochloric acid and NaOH (1 N) were used. The studied variables were pH (3, 5, 7, 9 and 11), amount of magnetic nanocomposite (0.005, 0.01, 0.02, 0.03, 0.04, 0.05 and 0.1 g/L), initial concentration of humic acid (2, 5, 10 and 15 mg/L), contact time (5, 10, 15, 30, 60, 90 and 200 min) and concentration of hydrogen peroxide (50, 100, 150 and 200 mg/L).

The samples were removed on predetermined intervals, and the remaining concentration of humic acid was evaluated using a spectrophotometer (UV/Visible T80⁺) at 254 nm. In the samples including hydrogen peroxide, the 0.2 N $Na_2S_2O_3$ solution was used immediately after removing the sample in order to minimize the confounding effect of H_2O_2 on the results. Eq. (1) was employed to calculate the efficiency of the adsorption process:

$$Y\% = \left[\frac{(HA_0 - HA_t)}{HA_0} \right] \times 100 \quad (1)$$

where HA_0 and HA_t , respectively, denote the initial and final concentrations of humic acid (mg/L). To examine the catalytic processes for water treatment, it is essential to use reaction rate kinetics. The rate of heterogeneous catalytic reactions is usually described using the pseudo-first-order (PFO) kinetic model and can be explained in the conditions of Langmuir–Hinshelwood (L-H) kinetic model [30–32].

$$r = k' \theta = -\frac{dC}{dt} = k' \left(\frac{KC}{1+KC} \right) \quad (2)$$

Here, r is the initial reaction rate (mg/L min), k' is the reaction rate constant, C denotes pollutant concentration (mg/L), K shows adsorption coefficient and θ indicates reactant site for the nanocomposite surface covered by HA. For very-low-concentration solutions (e.g., medications in water) with $KC \ll 1$, the L-H equation (Eq. (1)) is simplified to a PFO kinetic rule:

$$\frac{dC}{dt} = k_{obs} C \quad (3)$$

$$\ln \left(\frac{C}{C_0} \right) = -k_{obs} t \quad (4)$$

Here, k_{obs} is the observed PFO reaction rate constant (min^{-1}), t denotes reaction time (min), C is the remaining concentration after a specified time and C_0 is the pollutant's initial concentration (mg/L).

3. Results and discussion

3.1. Properties of the synthesized nanocomposite

To examine the properties of the synthesized nanocomposite, TEM, FESEM, FTIR and VSM spectra were employed. The following figures illustrate the results.

Fig. 2(a) shows the FTIR spectrum for the $FeNi_3@SiO_2$ sample. The peak at 479 cm^{-1} was related to the vibrations of Fe–Ni and another peaks at 669, 804, 972 cm^{-1} assigned to Ni–Fe–Ni or Fe–Ni–Ni bond.

The vibrations at 669.69, 804.54 and $1,124.05 \text{ cm}^{-1}$ were related to the Si–O–Si group and at 972.08 peak assigned to

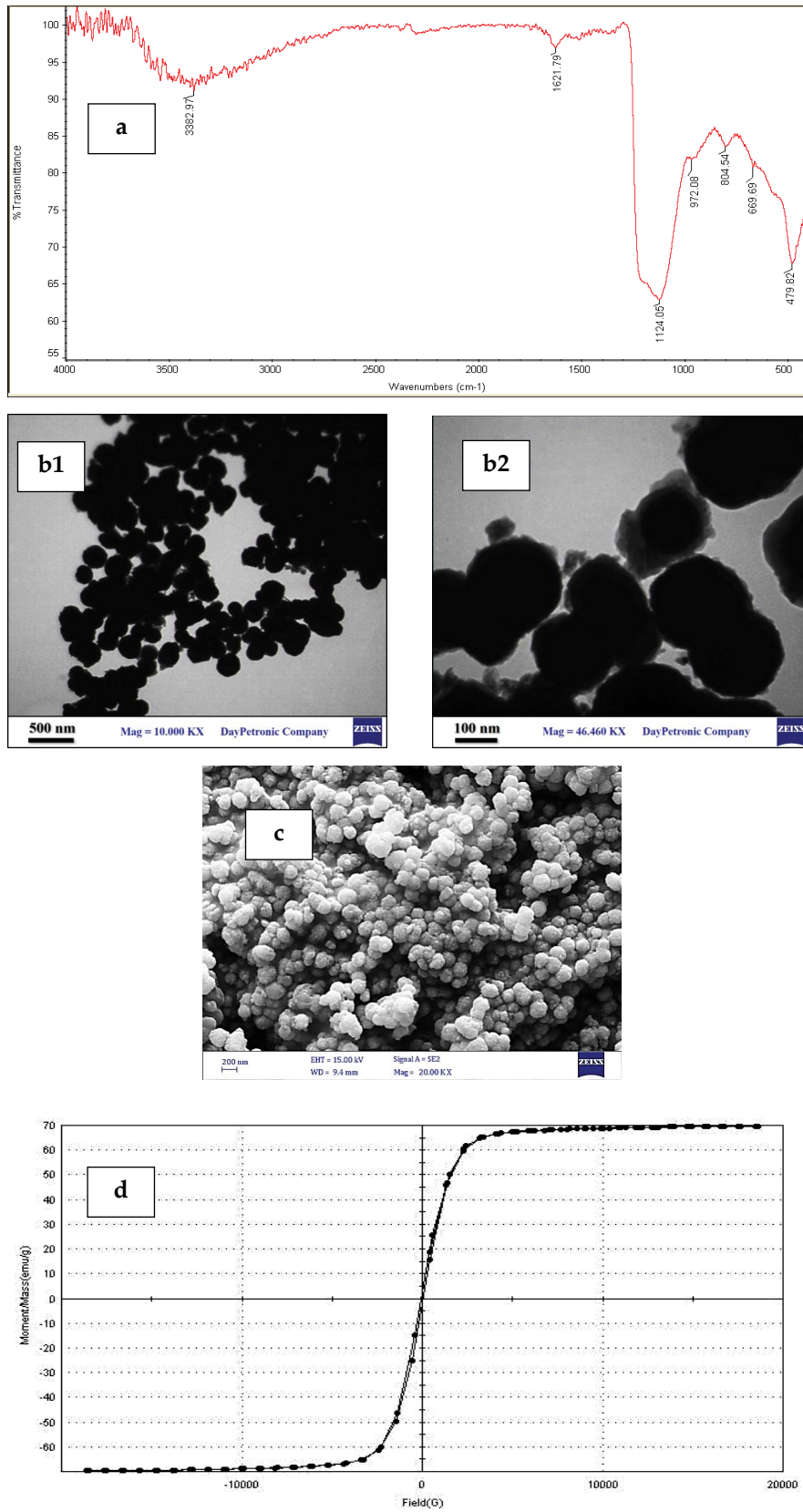


Fig. 2. Properties of the FeNi₃@SiO₂ magnetic nanoparticle: (a) FTIR, (b) TEM, (b1 = FeNi₃) and (b2 = FeNi₃@SiO₂), (c) SEM and (d) magnetic hysteresis loop.

Si–O–H stretching vibration. The weak adsorption band at $3,382.27\text{ cm}^{-1}$ belonged to the hydroxyl group (O–H) band vibration [33].

The structure and morphology of the FeNi_3 and $\text{FeNi}_3@$ SiO_2 were investigated by TEM images (Fig. 2(b1)) and (Fig. 2(b2)). As shown, aggregated and spherical nanoparticles were with size about 45 nm. Based on the TEM image, the SiO_2 cover was placed successfully on the FeNi_3 nanoparticle. FESEM image (Fig. 2(c)) illustrates the morphology and structure of the synthesized magnetic nanoparticles. Based on the FESEM image, it is indicated that microsphere surface of $\text{FeNi}_3@$ SiO_2 was porous and rough, and therefore, have a suitable catalytical and magnetical property. Also, FeNi_3 was encapsulated in the core of SiO_2 [34].

The magnetic property of the $\text{FeNi}_3@$ SiO_2 nanocomposite was studied using VSM at 300 K. Based on Fig. 2(d), the $\text{FeNi}_3@$ SiO_2 nanoparticle had super paramagnetic properties. Its saturation magnetization equalled 69.69 (electrostatic unit/g). Therefore, it can be easily separated in the presence of an external magnetic field.

3.2. Humic acid adsorption and degradation

This phase was done in two separate steps (adsorption removal and Fenton-like degradation of humic acid).

3.2.1. Humic acid adsorption test ($\text{FeNi}_3@$ SiO_2)

In order to determine the equilibrium time of the $\text{FeNi}_3@$ SiO_2 process, batch adsorption experiments were performed in the pH range of 3, 5, 7, 9 and 11; nanoparticle dose (0.005–0.1 g/L); humic acid initial concentration of 2–15 mg/L and contact time of 5–180 min. Results showed that the highest humic acid adsorption percentage was 99.8 at the concentration of 10 mg/L, pH = 3, nanoparticle dosage of 0.1 g/L and time of 180 min.

By increasing pH from 3 to 11, the removal percentage was decreased from 34% to 19% at 0.02 g/L of $\text{FeNi}_3@$ SiO_2 adsorbent, time of 60 min and concentration of 10 mg/L. Similar results were obtained by Asgari et al. [9,35,36]. This study demonstrated that by increasing pH from 2 to 10, humic acid removal percentage was decreased [37]. The decrease in adsorption rate may be related to the anionic structure of humic acid and pH_{ZPC} of the adsorbent. At the pH equal to pH_{ZPC} , the electrical charge of the adsorbent surface is in equilibrium with the environment. However, at the pH higher or less than pH_{ZPC} , the electrical charge of this surface is negative and positive, respectively. In this study, the pH_{ZPC} of the nanoparticle equalled 7.5. At higher pH levels, the dominant charge on the adsorbent surface was negative due to the aggregation of OH anions. Since humic acid has an anionic nature, its adsorption rate is reduced in alkaline conditions. The aggregation of negative charges on adsorbent surface causes a repulsion force between the pollutant and the adsorbent, thereby reducing adsorption rate. Moreover, in alkaline environments, proton is released and the complete ionization of humic acid to anions is increased, thereby highly decreasing adsorption rate [9,35,36,38,39]. Removal efficiency is affected by these conditions which are related to the anionic or cationic status of the pollutant [40,41]. At the pH levels lower than 3, the concentration of hydroxonium

ions is increased in the solution, preventing the adsorption of the pollutant by active sites on the adsorbent surface. Similar results were obtained in this study, and pH = 3 was selected for adsorption experiments.

Based on Fig. 3, by increasing the dosage of $\text{FeNi}_3@$ SiO_2 from 0.005 to 0.1 g/L during the initial 10 mg/L concentration, the remaining concentration of humic acid was reduced from 82% to 38%, with small changes in the remaining concentration after this time. These phenomena could be due to the improvement exchange sites on the adsorbent surface, equilibrium time equalled 60 min in the adsorption process. In addition to increasing the initial concentration of humic acid (from 2 to 15 mg/L), adsorption percentage was decreased (from 97.71% to 64.21%) at 60 min, which is due to $\text{FeNi}_3@$ SiO_2 adsorbent has a limited active site that at high humic acid concentration, these sites could saturate faster. According to BET results, $\text{FeNi}_3@$ SiO_2 synthesized has a surface area of $481.58\text{ m}^2/\text{g}$ and its total pore volume was of $0.2\text{ cm}^3/\text{g}$.

3.2.2. Fenton-like catalytic process for humic acid degradation ($\text{FeNi}_3@$ $\text{SiO}_2/\text{H}_2\text{O}_2$)

3.2.2.1. Effect of pH

Fig. 4 indicates the results of examining the effect of pH by $\text{FeNi}_3@$ SiO_2 magnetic nanoparticles separately and with hydrogen peroxide ($\text{FeNi}_3@$ $\text{SiO}_2/\text{H}_2\text{O}_2$) Fenton-like catalytic system). Results showed that pH had a significant effect on the removal efficiency of humic acid in both processes and these results are shown in Fig. 5. According to this figure, the efficiency of humic acid removal was 58.5% by the $\text{FeNi}_3@$ $\text{SiO}_2/\text{H}_2\text{O}_2$ Fenton-like system at pH = 7 as the optimal pH and 34% by $\text{FeNi}_3@$ SiO_2 magnetic nanoparticles alone at pH = 3 as the optimal adsorption pH. Contrary to the normal Fenton process ($\text{Fe}^{2+}-\text{H}_2\text{O}_2$) which is increased at acidic pH levels (2–3), the Fenton-like catalytic process using $\text{FeNi}_3@$ SiO_2 magnetic nanoparticles had a lower efficiency in this condition. At alkaline pH levels, H_2O_2 was decomposed into H_2O and O_2 , and the production of active-free radicals was decreased compared with acidic and neutral conditions [23].

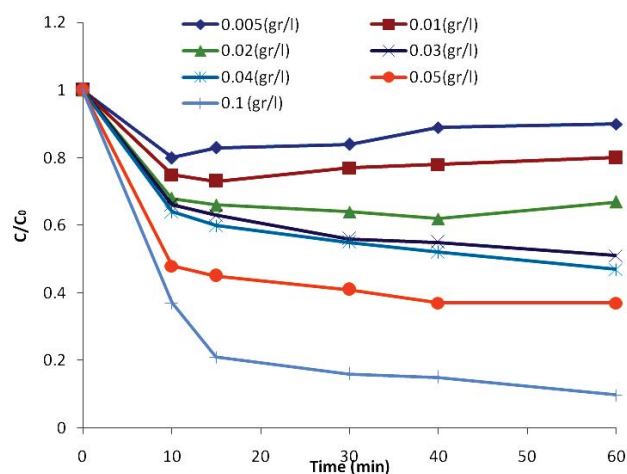


Fig. 3. Effect of $\text{FeNi}_3@$ SiO_2 magnetic nanocomposite dosage on the adsorption of humic acid (pH = 3 and humic acid initial concentration = 10 mg/L).

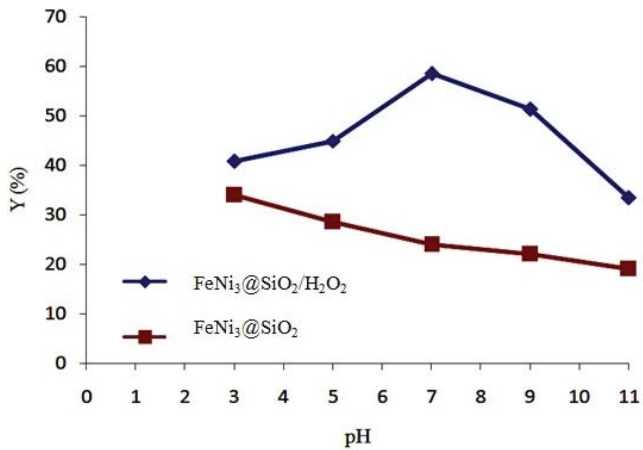


Fig. 4. Effect of initial pH of the solution on the removal of humic acid (concentration = 10mg/L) in two processes: adsorption with FeNi₃@SiO₂ (dose = 0.02 g/L) and FeNi₃@SiO₂/H₂O₂ heterogeneous catalytic Fenton-like process (FeNi₃@SiO₂ dose = 0.02 g/L, H₂O₂ = 150 mg/L).

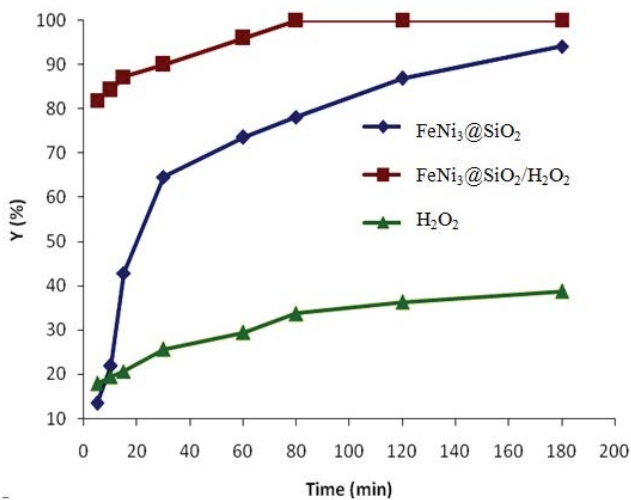


Fig. 5. Comparing humic acid removal using various processes at their optimum pH (FeNi₃@SiO₂ pH = 3, FeNi₃@SiO₂/H₂O₂ pH = 7, H₂O₂ pH = 11).

In alkaline pH conditions, the humic acid removal percentage in FeNi₃@SiO₂ and FeNi₃@SiO₂/H₂O₂ was respectively 11% and 33.4% at pH = 11, and 34% and 40.76% at pH = 3. Thus, it is clear that the FeNi₃@SiO₂/H₂O₂ heterogeneous Fenton-like catalytic process had higher efficiency at neutral pH levels, which is an advantage since it requires no pH regulation or external energy source. This may be due to the changes in the catalyst's structural mechanism. A similar phenomenon has been reported in other studies [18,23]. Nevertheless, the mechanism of these changes needs further research. The optimal neutral pH can be related to the SiO₂ cover on the FeNi₃ nanoparticle [18,42].

The p*H*_{ZPC} of the FeNi₃@SiO₂ magnetic nanoparticle was about 7.5. At higher pH levels, the hydroxyl groups in the SiO₂ were deprotonated, generated ⁻OH, and their surface charge was negative. Moreover, the reduction in pH produced ⁻OH₂⁺,

making the surface charge positive. Thus, at lower pH levels, the ⁻OH₂⁺ repulsed humic acid from the nanoparticle surface because of the electrostatic repulsion force. At high pH levels, the lack of proton stopped the Fenton-like reaction. At the optimal pH, close to the p*H*_{ZPC} of FeNi₃@SiO₂, OH hydroxyl groups could create chelation and promote the efficiency of the process.

Results of this study were in line with those by Huang et al. [23] on the removal of bisphenol by Fe₃O₄ magnetic nanoparticles in the heterogeneous Fenton-like catalytic process; Yang et al. [18,27] on Fe₃O₄@SiO₂ nanoparticles in a Fenton-like system and Liu et al. [26] on the removal of dye discoloration by Fe₃O₄/TiO₂/C magnetic nanoparticles in a Fenton-like catalytic system. Wang et al. [16] examined the use of Fe₃O₄@SiO₂/C nanocomposite for the removal of methylene blue, showing that the optimal conditions for this nanocomposite together with H₂O₂ (catalytic Fenton-like) were neutral conditions. Ghaneian et al. [43] reported similar results in investigating the catalytic oxidation process of humic acid.

3.2.2.2. Effect of the amount of magnetic nanocomposite and contact time

To examine the effect of magnetic nanocomposite dosage, the experiments were evaluated at the dosage of 0.005–0.1 g/L, pH = 7, H₂O₂ concentration of 150 mg/L and humic acid concentration of 10 mg/L. Fig. 6 shows the diagram of humic acid destruction in the presence of FeNi₃@SiO₂/H₂O₂ using various doses of the FeNi₃@SiO₂ nanocatalyst. Based on this figure, the pollutant removal percentage was enhanced by increasing the dose in the FeNi₃@SiO₂/H₂O₂ Fenton-like catalytic process. Removal efficiency equalled 54.18% and 100% at the doses of 0.005 and 0.1 g/L, respectively. Using H₂O₂ alone, the maximum removal percentage of 38.71 was obtained at its highest concentration (200 mg/L). Fig. 5 clearly shows the effect of simultaneously using the magnetic nanoparticle and H₂O₂, as the SiO₂ cover enhanced the catalytic activity of FeNi₃. Thus, this nanoparticle acts as a peroxidase-like catalyst to accelerate the decomposition of H₂O₂

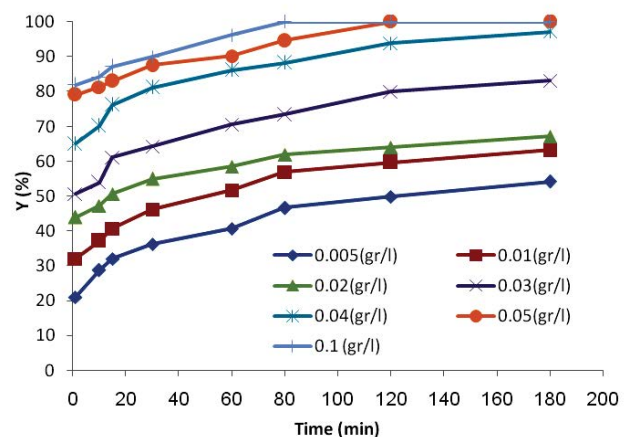


Fig. 6. Effect of the concentration of FeNi₃@SiO₂/H₂O₂ nanocomposite on the removal of humic acid (pH = 7, humic acid concentration of 10 mg/L and H₂O₂ concentration of 150 mg/L).

and turn it into OH[•] radicals [16]. Although the magnetic core of FeNi₃ alone has a similar specific surface area to FeNi₃@SiO₂, it has no catalytic activity alone in decomposing H₂O₂ at nearly neutral pH levels, but SiO₂ cover could promote its catalytic activity in Fenton-like catalytic process.

When the dose of FeNi₃/SiO₂ was increased from 0.005 to 0.1 mg/L, the destruction rate constant (K_{obs}) was significantly increased from 0.0044 to 0.026 min⁻¹ (Fig. 7). Yang et al. studied the Fe₃O₄@SiO₂ catalytic nanoparticle for the removal of methylene blue and reported similar results [16]. This comparison clearly showed that the SiO₂ cover was essential for promoting the catalytic process. SiO₂ can improve this process by several methods. First, amorphous SiO₂ can lead to the adsorption of humic acid around the surface of FeNi₃. Therefore, when free radicals are created, they attack the humic acid molecule before automatic destruction. Second, SiO₂ may prove useful in electron exchange. Third, the hydroxyl groups in SiO₂ may chelate Fe²⁺/Fe³⁺ on the surface of FeNi₃. Numerous studies have shown that chelating promotes the catalytic process of FeNi₃ [16,18]. SiO₂ has many hydroxyl groups on its surface. These groups can chelate Fe²⁺ and Fe³⁺ ions.

3.2.2.3. Effect of contact time and humic acid initial concentration

In the removal of humic acid, the examined initial concentration was in the range of 2–15 mg/L at pH = 7 with the catalyst dose of 0.02 g/L and H₂O₂ concentration of 150 mg/L. Fig. 8 shows that by increasing the initial concentration of humic acid, removal percentage decreased. At the initial concentrations of 2 and 15 mg/L, removal concentration equalled 100% and 89.46%, respectively, at the time of 60 min, after which the removal percentage had no significant increase. The reduction in removal percentage caused by the increase in humic acid initial concentration can be justified as follows: since the amount of FeNi₃@SiO₂ catalyst, contact time, pH and H₂O₂ concentration were equal at all concentrations, the amount of generated radical was the same at all the four concentrations. Therefore, humic acid removal would be higher in the samples with lower concentrations [44,45].

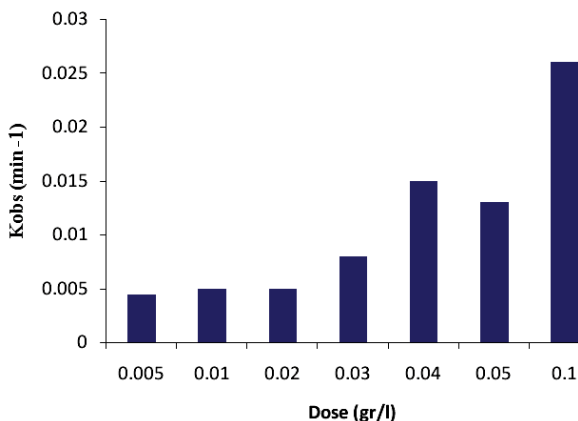


Fig. 7. Kinetics of the effect of FeNi₃@SiO₂ magnetic nanocomposite dose on the removal of humic acid (initial concentration of 10 mg/L, pH = 7 and H₂O₂ concentration of 150 mg/L).

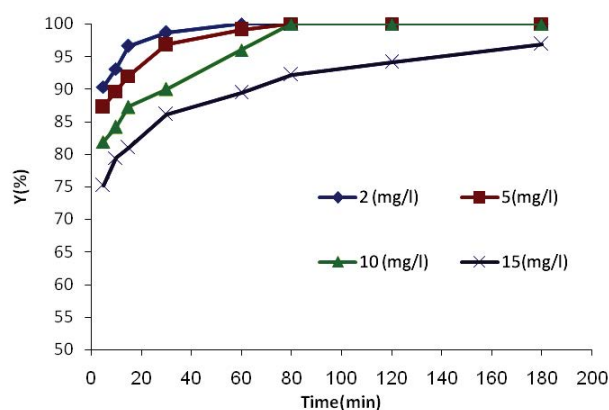


Fig. 8. Effect of humic acid initial concentration in the Fenton-like catalytic process (FeNi₃@SiO₂ magnetic nanocomposite dose of 0.1 g/L, pH = 7 and H₂O₂ concentration of 150 mg/L).

According to Fig. 9, by increasing the initial concentration of humic acid, the reaction rate constant was reduced from 0.077 to 0.022 min⁻¹, which could be due to the transformation from the regime of the kinetic control at low concentrations to mass transfer restriction at high concentrations [45]. Furthermore, at high concentrations, more humic acid molecules were adsorbed on the surface of the nanocatalyst. The increased amount of humic acid adsorption had an inhibitory effect in its reaction with hydroxyl radicals due to the reduction in the direct time between them [45]. In all the cases, the correlation coefficient (R^2) was higher than 0.90, indicating that the results of the experiments were compatible with the PFO kinetic model. Results of this study were consistent with those of previous works [30,45,46].

3.2.2.4. Effect of H₂O₂ concentration

Adding hydrogen peroxide to the heterogeneous Fenton-like catalytic process (FeNi₃@SiO₂/H₂O₂) results in an increase in the catalytic oxidation rate in most cases. To maintain the efficiency of the added H₂O₂, it is necessary to select the H₂O₂ concentration based on the type and concentration of the pollutant [46]. To study the effect of H₂O₂ in the Fenton-like system, the dose of FeNi₃@SiO₂ was 0.1 g/L at pH = 7, humic acid

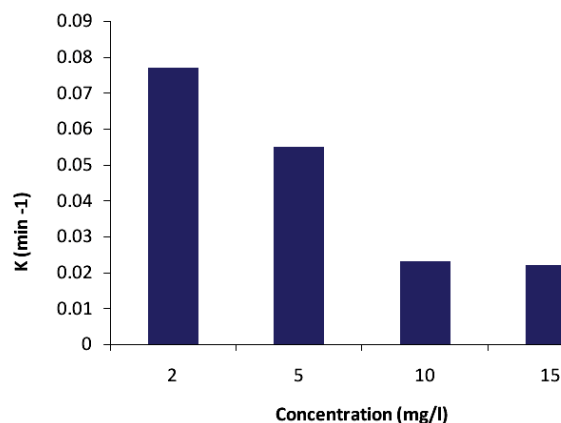
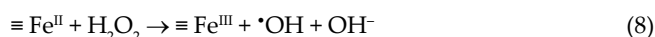
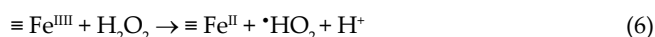


Fig. 9. Kinetics of humic acid removal at different concentrations.

initial concentration of 10 mg/L and H₂O₂ concentrations of 50, 100, 150 and 200 mg/L. According to Fig. 10, the best dose of H₂O₂ was 200 mg/L. By increasing the concentration of H₂O₂, removal efficiency increased. These results were in line with those by Yazdanbakhsh et al. [37] on the removal of humic acid in a peroxi-electrocoagulation process. Accordingly, by increasing the H₂O₂ concentration from 50 to 200 mg/L, the destruction of humic acid was increased to 100%. In all the experimental conditions, the kinetic of humic acid reduction followed a PFO model. By increasing the H₂O₂ concentration, the reaction rate constant (K_{obs}) was significantly increased from 0.013 to 0.0281 min⁻¹. Similar results have been reported by Huang et al. [23] on the catalytic destruction of bisphenol. Moreover, Lou et al. [12] found similar results in the process of removing humic acid using UV/H₂O₂.

The removal percentage of humic acid at the time of 60 min and initial concentration of 10 mg/L was 29.4% using H₂O₂ alone, 73.64% in the FeNi₃@SiO₂ nanoparticle process and 96.02% in the FeNi₃@SiO₂/H₂O₂ Fenton-like catalytic system, indicating the increased catalytic activity of the magnetic nanoparticle in the presence of H₂O₂. H₂O₂ through production-free radicals, such as •OH, could attack organic compounds relatively nonselectively and oxidizes these compounds by abstraction of hydrogen atom or by addition to double bonds. One of the major reasons for this increase is the production of more free radicals at higher oxidant concentrations. The suggested mechanism for the heterogeneous Fenton-like system in iron-containing catalysts is in the form of the following reactions [24].



It must be noted that it is necessary to determine the optimal amount of hydrogen peroxide in the heterogeneous Fenton-like catalytic process (FeNi₃@SiO₂/H₂O₂) because (1) by increasing the concentration of hydrogen peroxide, costs will increase; (2) by increasing the H₂O₂ concentration, the

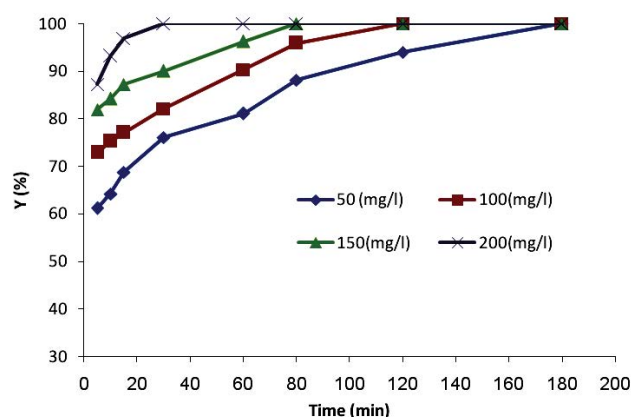


Fig. 10. Effect of H₂O₂ concentration in the catalytic process of humic acid removal.

production of hydroxyl radical is somewhat reduced (H₂O₂ acts as a hydroxyl scavenger according to Eqs. (9) and (10) and (3) it increases the chemical oxygen demand in the sample because of the presence of the remaining H₂O₂ [18,46].



While the degradation pathway has not been investigated in this study, but it has been reported in another study that small carboxylic acids such as oxalic, maleic, formic and acetic acids are common oxidation products of larger humic acid molecules after degradation and fragmentation. Oxalic acid is easily degraded with hydroxyl radicals, but carboxylic acids that remained, especially acetic acids, react weakly with OH radicals [47,48].

4. Conclusion

In brief, the synthesized FeNi₃@SiO₂ magnetic nanocomposite had high efficiency in the Fenton-like catalytic process. This treatment method did not have the disadvantages of the heterogeneous Fenton system and could be used as an effective process for the quick removal of humic acid in different environments, especially the neutral ones, with high efficiency. Some interesting properties of the FeNi₃@SiO₂ Fenton-like catalyst were as follows:

(1) use in the environments with neutral pH; (2) resistance against radical scavengers; (3) quick kinetics; (4) simple separation using magnetic field and (5) reusability.

The best conditions for removing humic acid in this system included: pH = 7, nanoparticle dose of 0.1 g/L, H₂O₂ concentration of +200 mg/L and time of 60 min. The kinetic removal followed the PFO kinetic equation. The results revealed that this system had a good potential for destroying humic acid. Also, this nanocomposite could be used together with H₂O₂ as an economical and efficient method.

Acknowledgement

The authors would like to express their thanks to the laboratory staff and faculty member of the Department of Environmental Health Engineering, School of Public Health, Birjand University of Medical Sciences for their collaboration.

References

- [1] S. Metsämuuronen, M. Sillanpää, A. Bhatnagar, M. Mänttari, Natural organic matter removal from drinking water by membrane technology, *Sep. Purif. Rev.*, 43 (2014) 1–61.
- [2] M. Zazouli, S. Nasser, A.H. Mahvi, M. Gholami, A. Mesdaghinia, M. Younesian, Retention of humic acid from water by nanofiltration membrane and influence of solution chemistry on membrane performance, *J. Environ. Health. Sci. Eng.*, 5 (2008) 11–18.
- [3] A.F. Ashery, K. Radwan, M. Rashed, The Effect of pH Control on Turbidity and NOM Removal in Conventional Water Treatment, *Proceedings of the Fifteen International Water Technology Conference, Alexandria, Egypt, 2011.*
- [4] A. Matilainen, *Removal of the Natural Organic Matter in the Different Stages of the Drinking Water Treatment Process*, Tampereen teknillinen yliopisto Julkaisu-Tampere University of Technology Publication, 2007, p. 651.

- [5] M.V. Niri, A.H. Mahvi, M. Alimohammadi, M. Shirardi, H. Golastanifar, M.J. Mohammadi, A. Naeimabadi, M. Khishdost, Removal of natural organic matter (NOM) from an aqueous solution by NaCl and surfactant-modified clinoptilolite. *J. Water Health*, 13 (2015) 394–405.
- [6] J. Lowe, M.M. Hossain, Application of ultrafiltration membranes for removal of humic acid from drinking water, *Desalination*, 218 (2008) 343–354.
- [7] Y. Wang, J. Le Roux, T. Zhang, J.-P. Croué, Formation of brominated disinfection byproducts from natural organic matter isolates and model compounds in a sulfate radical-based oxidation process, *Environ. Sci. Technol.*, 24 (2014) 14534–14542.
- [8] E. Bazrafshan, H. Biglari, A.H. Mahvi, Humic acid removal from aqueous environments by electrocoagulation process using iron electrodes, *E-J. Chem.*, 9 (2012) 2453–2461.
- [9] G. Asgari, A. Ebrahimi, A.S. Mohammadi, G. Ghanizadeh, The investigation of humic acid adsorption from aqueous solutions onto modified pumice with hexadecyl trimethyl ammonium bromide, *Int. J. Environ. Health Eng.*, 2 (2013) 2–20.
- [10] M.H. Amin, M. Safari, R. Rezaee, Investigating the efficiency of enhanced coagulation process for the removal of humic substances from water, *J. Environ. Sci. Technol.*, 18 (2016) 157–165.
- [11] S. Moussavi, M. Ehrampoush, A. Mahvi, M. Ahmadian, S. Rahimi, Adsorption of humic acid from aqueous solution on single-walled carbon nanotubes, *Asian J. Chem.*, 25 (2013) 5319–5324.
- [12] X. Lou, D. Xiao, C. Fang, Z. Wang, J. Liu, Y. Guo, L. Shuyn, Comparison of UV/hydrogen peroxide and UV/peroxydisulfate processes for the degradation of humic acid in the presence of halide ions, *Environ. Sci. Pollut. Res. Int.*, 23 (2016) 4778–4785.
- [13] D.A. Fearing, J. Banks, S. Guyetand, C.M. Eroles, B. Jefferson, D. Wilson, P. Hillis, A.T. Campbell, S.A. Parsons, Combination of ferric and MIEX® for the treatment of a humic rich water, *Water Res.*, 38 (2004) 2551–2558.
- [14] Z. Ke-xin, R. Hong-wei, X. Shu-guang, Performance of combined pre-ozonation and biofiltration for the purification of water from ching yellow river, *J. Environ. Sci.*, 1 (2007) 52–61.
- [15] K. Babi, K. Koumenides, A. Nikolaou, C. Makri, F. Tzoumerkas, T. Lekkas, Pilot study of the removal of THMs, HAAs and DOC from drinking water by GAC adsorption, *Desalination*, 210 (2007) 215–224.
- [16] R. Wang, X. Liu, R. Wu, B. Yu, H. Li, X. Zhang, J. Xie, S.-T. Yang, $\text{Fe}_3\text{O}_4/\text{SiO}_2/\text{C}$ nanocomposite as a high-performance Fenton-like catalyst in a neutral environment, *RSC Adv.*, 6 (2016) 8594–8600.
- [17] R. Rezaee, A. Maleki, A. Jafari, S. Mazloomi, Y. Zandsalimi, A.H. Mahvi, Application of response surface methodology for optimization of natural organic matter degradation by UV/ H_2O_2 advanced oxidation process, *J. Environ. Health Sci. Eng.*, 12 (2014) 1–8.
- [18] S.-T. Yang, W. Zhang, J. Xie, R. Liao, X. Zhang, B. Yu, R. Wu, X. Liu, H. Li, Z. Guo, $\text{Fe}_3\text{O}_4/\text{SiO}_2$ nanoparticles as a high-performance Fenton-like catalyst in a neutral environment, *RSC Adv.*, 5 (2015) 5458–5463.
- [19] R. Huang, Z. Fang, X. Fang, E.P. Tsang, Ultrasonic Fenton-like catalytic degradation of bisphenol A by ferrous oxide (Fe_2O_3) nanoparticles prepared from steel pickling waste liquor, *J. Colloid Interface Sci.*, 436 (2014) 258–266.
- [20] S. Valizadeh, M. Rasoulifard, M.S. Dorraji, Modified Fe_3O_4 -hydroxyapatite nanocomposites as heterogeneous catalysts in three UV, Vis and Fenton like degradation systems, *Appl. Surf. Sci.*, 319 (2014) 358–366.
- [21] R. Guo, L. Fang, W. Dong, F. Zheng, M. Shen, Magnetically separable BiFeO_3 nanoparticles with a $\gamma\text{-Fe}_2\text{O}_3$ parasitic phase: controlled fabrication and enhanced visible-light photocatalytic activity, *J. Mater. Chem.*, 21 (2011) 18645–18652.
- [22] Z.-T. Hu, B. Chen, T.-T. Lim, Single-crystalline $\text{Bi}_2\text{Fe}_4\text{O}_{13}$ synthesized by low-temperature co-precipitation: performance as photo- and Fenton catalysts, *RSC Adv.*, 4 (2014) 27820–27829.
- [23] R. Huang, Z. Fang, X. Yan, W. Cheng, Heterogeneous sono-Fenton catalytic degradation of bisphenol A by Fe_3O_4 magnetic nanoparticles under neutral condition, *Chem. Eng.*, 197 (2012) 242–249.
- [24] W. Luo, L. Zhu, N. Wang, H. Tang, M. Cao, Y. She, Efficient removal of organic pollutants with magnetic nanoscaled BiFeO_3 as a reusable heterogeneous Fenton-like catalyst, *Environ. Sci. Technol.*, 44 (2010) 1786–1791.
- [25] X. Zhang, M. He, J.-H. Liu, R. Liao, L. Zhao, J. Xie, R. Wang, S.T. Yang, H. Wang, Y. Liu, $\text{Fe}_3\text{O}_4/\text{C}$ nanoparticles as high-performance Fenton-like catalyst for dye decoloration, *Chinese. Sci. Bull.*, 59 (2014) 3406–3412.
- [26] X. Liu, Q. Zhang, B. Yu, R. Wu, J. Mai, R. Wang, L. Chen, S.T. Yang, Preparation of $\text{Fe}_3\text{O}_4/\text{TiO}_2/\text{C}$ nanocomposites and their application in Fenton-Like catalysis for dye decoloration, *Catalysts*, 6 (2016) 146.
- [27] S. Yang, L. Yang, X. Liu, J. Xie, X. Zhang, B. Yu, R. Wu, H.L. Li, L.Y. Chen, J. Liu, TiO_2 -doped Fe_3O_4 nanoparticles as high-performance Fenton-like catalyst for dye decoloration, *Sci. China Technol. Sci.*, 58 (2015) 858–863.
- [28] M.A. Nasser, S.M. Sadeghzadeh, A highly active $\text{FeNi}_3\text{-SiO}_2$ magnetic nanoparticles catalyst for the preparation of 4H-benzo [b] pyrans and Spirooxindoles under mild conditions. *J. Iran. Chem. Soc.*, 10 (2013) 1047–1056.
- [29] X. Ding, Y. Huang, M. Zong, Synthesis and microwave adsorption enhancement property of core-shell $\text{FeNi}_3/\text{SiO}_2$ -decorated reduced graphene oxide nanosheets. *Mater. Lett.*, 157 (2015) 285–289.
- [30] A. Eslami, M.M. Amini, A.R. Yazdanbakhsh, A. Mohseni-Bandpei, A.A. Safari, A. Asadi, N, S co-doped TiO_2 nanoparticles and nanosheets in simulated solar light for photocatalytic degradation of non-steroidal anti-inflammatory drugs in water: a comparative study, *J. Chem. Technol. Biotechnol.*, 91 (2016) 2693–2704.
- [31] V. Kitsiou, N. Filippidis, D. Mantzavinos, I. Poullos, Heterogeneous and homogeneous photocatalytic degradation of the insecticide imidacloprid in aqueous solutions, *Appl. Catal.*, B, 86 (2009) 27–35.
- [32] A. Khanna, V.K. Shetty, Solar light induced photocatalytic degradation of Reactive Blue 220 (RB-220) dye with highly efficient $\text{Ag}@\text{TiO}_2$ core-shell nanoparticles: a comparison with UV photocatalysis, *Solar Energy*, 99 (2014) 67–76.
- [33] X. Ding, Y. Huang, J. Wang, H. Wu, P. Liu, Excellent electro-magnetic wave adsorption property of quaternary composites consisting of reduced graphene oxide, polyaniline and $\text{FeNi}_3/\text{SiO}_2$ nanoparticles, *Appl. Surf. Sci.*, 357 (2015) 908–914.
- [34] R. Wang, X. Wang, X. Xi, R. Hu, G. Jiang, Preparation and photocatalytic activity of magnetic $\text{Fe}_3\text{O}_4/\text{SiO}_2/\text{TiO}_2$ composites, *Adv. Mater. Sci. Eng.*, 2012 (2012) 1–8.
- [35] T. Anirudhan, M. Ramachandran, Surfactant-modified bentonite as adsorbent for the removal of humic acid from wastewaters, *Appl. Clay Sci.*, 35 (2007) 276–281.
- [36] S.-G. Wang, W.-X. Gong, X.-W. Liu, B.-Y. Gao, Q.-Y. Yue, D.-H. Zhang, Removal of fulvic acids from aqueous solutions via surfactant modified zeolite 11 supported by the National High-tech and Development of Program of China (No. 2003AA601060), *Chem. Res. Chinese Univ.*, 22 (2006) 566–5670.
- [37] A.R. Yazdanbakhsh, M. Kermani, S. Komasi, E. Aghayani, A. Sheikhmohammadi, Humic acid removal from aqueous solutions by peroxi-electrocoagulation process, *Environ. Health Eng. Manage. J.*, 2 (2015) 53–58.
- [38] B. Hameed, A. Ahmad, N. Aziz, Isotherms, kinetics and thermodynamics of acid dye adsorption on activated palm ash, *Chem. Eng.*, 133 (2007) 195–203.
- [39] H. Tashauoei, H.M. Attar, M. Amin, M. Kamali, M. Nikaen, M.V. Dastjerdi, Removal of cadmium and humic acid from aqueous solutions using surface modified nanozeolite A, *Int. J. Environ. Sci. Technol.*, 7 (2010) 497–508.
- [40] Gh. Asgari, Gh. Ghanizadeh, A. Seydmohammadi, Adsorption of humic acid from aqueous solutions onto modified pumice with hexadecyl trimethyl ammonium bromide, *J. Babol Univ. Med. Sci.*, 14 (2011) 14–22.
- [41] M. Kitis, E. Karakaya, N.O. Yigit, G. Civelekoglu, A. Akcil, Heterogeneous catalytic degradation of cyanide using copper-impregnated pumice and hydrogen peroxide, *Water Res.*, 39 (2005) 1652–1662.

- [42] J. Zhang, T. Yao, C. Guan, N. Zhang, H. Zhang, X. Zhang, J. Wu, One-pot preparation of ternary reduced graphene oxide nanosheets/Fe₂O₃/polypyrrole hydrogels as efficient Fenton catalysts, *J. Colloid Interface Sci.*, 505 (2017) 130–138.
- [43] M. Ghaneian, M. Ehrampoush, M. Dehvari, M. Kheirkhah, F. Anvar, M. Askarshahi, B. Jamshidi, The investigation of electron beam catalytical oxidation process efficiency with potassium persulfate in removal humic acid from aqueous solutions, *Toloo-E-Behdasht*, 14 (2015) 63–76.
- [44] R. Nosrati, A. Olad, R. Maramifar, Degradation of ampicillin antibiotic in aqueous solution by ZnO/polyaniline nanocomposite as photocatalyst under sunlight irradiation, *Environ. Sci. Pollut. Res. Int.*, 19 (2012) 2291–2299.
- [45] G. Safari, M. Hoseini, M. Seyedsalehi, H. Kamani, J. Jaafari, A. Mahvi, Photocatalytic degradation of tetracycline using nanosized titanium dioxide in aqueous solution, *Int. J. Environ. Sci. Technol.*, 12 (2015) 603–616.
- [46] M. Hoseini, Gh.H. Safari, H. Kamani, J. Jaafari, A.H. Mahvi, Survey on removal of tetracycline antibiotic from aqueous solutions by nano-sonochemical process and evaluation of the influencing parameters, *Iran. J. Health Environ.*, 8 (2015) 141–152.
- [47] S. Liu, M. Lim, K. Chiang, R. Amal, R. Fabris, C. Chow, M. Drikas, A study on the removal of humic acid using advanced oxidation processes, *Sep. Sci. Technol.*, 42 (2007) 1391–1404.
- [48] A.H. Mahvi, A. Maleki, R. Rezaee, M. Safari, Reduction of humic substances in water by application of ultrasound waves and ultraviolet irradiation, *Iran. J. Environ. Health Sci. Eng.*, 6 (2009) 233–240.